Photosynthesis Research (2023) 158:181–194
https://doi.org/10.1007/s11120-023-01045-7

RESEARCH

# Photosynthetic performance under adaxial and abaxial illumination in three Mediterranean *Quercus* species differing in branch architecture and individual leaf area

**Sonia Mediavilla**[1] · **Alfonso Escudero**[1]

Received: 30 May 2023 / Accepted: 14 August 2023 / Published online: 31 August 2023

**Abstract**
Light availability effects on canopy-level carbon balance constitute an especially difficult issue to address, owing to the strong spatial and temporal changes of the light environment within the canopy. One of the least explored aspects in relation to light environment is the interaction between leaf angle and leaf anatomy. The inclination of the leaf may affect the distribution of light between the adaxial and abaxial surface. The purpose of this study is determining the proportions of the leaf area receiving light from the abaxial side in branches of isolated trees in three Mediterranean oaks, as well as the photosynthetic responses to light under adaxial and abaxial illumination. The proportions of the leaf area illuminated from below were low for sun incidence angles near 0° with respect to the main axis of the branch. However, for sun incidence angles about 45°, the proportion of leaves receiving abaxial illumination was considerable. PPFD levels on the sunlit part of the abaxial surface were always lower than those in the upper leaf side, as a consequence of the lower projection efficiency for the leaves facing the sun by the lower side. Light absorptance was also lower on the abaxial side. The differences between both sides of the leaf tended to be stronger for thicker, longer-living leaves. We conclude that mean C assimilation of the canopy is significantly decreased by the presence of leaves facing the sun by the lower side and that this decrease is stronger in evergreen species with thicker leaves.

**Keywords** Light absorptance · Photosynthetic parameters · Adaxial and abaxial leaf surfaces · Leaf inclination · Branch architecture

## Introduction

In the current context of climate change, determining the carbon sequestration capacity of different tree species and its changes in response to the new conditions has become a priority research topic. However, the development of carbon balance models in tree species is complex because it requires a detailed measurement of how different environmental factors affect the assimilation of $CO_2$ by the different leaves in the crown of these species. Among others, the intensity of photosynthetically active radiation (PPFD) is a decisive factor for the carbon balance. However, its effects are especially difficult to incorporate into a model because the different species, depending on the geometry of their crown and the arrangement of their leaves (Fleck et al. 2003; Niinemets et al. 2004; Escudero et al. 2017), may show important differences in their light environment. For this reason, this is one of the worst-known carbon balance factors, because the measurement of space–time variations in the light environment is especially difficult in strongly branched tree species.

One of the least explored aspects in relation to light changes with the crown characteristics is the interaction between the leaf angle and the anatomy of the leaf (DeLucia et al. 1991; Myers et al. 1997; Valladares and Niinemets 2007). The inclination of the leaf affects the distribution of light between the adaxial and abaxial surface. When leaves exhibit strong dorsiventral asymmetry, there can be considerable differences in PPFD utilization patterns depending on the surface receiving the light. Bifacial leaves have a densely packed palisade mesophyll layer of cells on the adaxial side, and a more open layer of spongy mesophyll cells on the abaxial side, which has important implications

---

✉ Alfonso Escudero
ecoescu@usal.es

[1] Área de Ecología, Facultad de Biología, Universidad de Salamanca, Campus Unamuno s/n, 37071 Salamanca, Spain

on photosynthetic performance, with gas exchange rates usually higher when the leaf is illuminated on the adaxial compared to the abaxial surface (Terashima and Saeki 1985; Evans et al. 1993; Sun and Nishio 2001; Paradiso and Marcellis 2012; Zhang et al. 2016). In fact, it has been proposed that the palisade is more efficient for photosynthesis than the spongy mesophyll, because of the combination of the higher concentrations of photosynthetic pigments and proteins, higher photosynthetic capacity and chloroplasts that have characteristics associated with acclimation to high irradiance (sun type vs. shade type of spongy mesophyll) and, finally, to a structure that allows a more efficient light utilization, with greater penetration and less light scattering than in the spongy mesophyll (Terashima and Saeki 1983; Vogelmann et al. 1996; Smith et al. 1997; Sun and Nishio 2001).

If we assume that carbon fixation is higher when the leaf is illuminated on the adaxial compared to the abaxial surface, it is to be expected that most of the leaves of a canopy should receive the light by the adaxial side (DeLucia et al. 1991; Valladares and Pearcy 1999). For this reason, most measurements and models on the photosynthetic performance of leaves have been made on leaves irradiated from the adaxial surface, since the contribution to the energy balance of the abaxial surface is considered to be minimal (Wang et al. 2008). However, within dense canopies, part of the leaves can receive light from the abaxial side either because of their arrangement or because they alter their orientation to minimize adverse environmental effects (Campbell et al. 2007; Paradiso and Marcelis 2012; Zhang et al. 2016). This situation must be especially frequent in open forests, where the trees receive solar radiation not only from above, but also from lateral positions. Different sides of the crown may receive sun radiation from different sun positions, which makes the light environment much more complex with respect to closed forests, where lateral illumination is more restricted (Sinoquet et al. 2007; Chen et al. 2008). Specifically, when describing the architecture of the crown of different species of *Quercus* in open forests, we found that, depending on the height of the sun, sometimes a significant part of the leaf surface appears illuminated by the underside (Escudero et al. 2017). This must have important implications on gas exchange rates that have hardly been studied so far. Assuming that light strikes exclusively the adaxial side could lead to unrealistic estimates of photosynthetic performance. Carbon balance at the canopy level should depend on how photosynthesis under adaxial and abaxial surfaces changes in each species, as well as on the proportion of leaf area that receives light on each side. However, as far as we know, there are hardly any studies that have incorporated the proportions of leaves that receive light on each surface to the estimates of canopy performance (Valladares and Pearcy 1999). One main reason for this lack of data is the fact that although different models have been developed (Pearcy and Yang 1996; Delagrange et al. 2006) that allow simulating the penetration of light into the crown, obtaining the necessary information is extremely time-consuming, especially in tree species of complex architecture (Delagrange et al. 2006; Sinoquet et al. 2007).

The present study focuses on three typical Mediterranean *Quercus* species (*Quercus faginea* Lam. *Q. suber* L. and *Q. ilex* L. subsp *ballota* (Desf.) Samp) known to differ in leaf life span and other leaf traits (Mediavilla and Escudero 2003; Gil-Pelegrín et al. 2017; Mediavilla et al. 2020). The leaves of the three species are dorsiventral, with pronounced differences between the palisade and the spongy mesophyll, hypostomatic and with a more or less dense layer of hairs on the abaxial side (Mediavilla et al. 2001, 2019). In a recent paper (Mediavilla and Escudero 2023), we have described the branch architectural traits of these same species. There were interspecific differences in leaf angle, shoot orientation, and internode length, among other architectural traits. These differences may be assumed to influence the leaf blade orientation with respect to the sun position. In the present paper, we propose first to analyze the spatial arrangement of the leaves of the three species to determine the proportion of leaf area of the canopy that receives light on each surface for different positions of the sun. And secondly, by analyzing gas exchange rates, we intend to determine whether there are differences in $CO_2$ assimilation between the two leaf surfaces and if they are of similar magnitude for the three species. Our ultimate goal is to incorporate the contribution of both types of leaves (those that receive light by the adaxial and by the abaxial side) to the final performance of each species. We will also analyze different leaf traits that could determine changes in the intensity of adaxial–abaxial differences between the three species and could help explain the results at the interspecific level. We hypothesize that photosynthetic performances in our three species will be lower under abaxial than under adaxial illumination and that the differences between both surfaces will increase with leaf thickness, because of the stronger dorsiventral asymmetry of the internal structure in thicker leaves.

## Materials and methods

### Study species and area

The study was carried out in a plot of the central west of Spain (with coordinates 41°08′49.02 ″N, 5°47′17.38 ″W), near the city of Salamanca, where specimens of the three analyzed species coexist. The plot has an altitude of about 830 m above sea level, a soil type dystric Cambisols, poor in organic matter and nutrients, with a low pH and medium/low water retention capacity (Dorronsoro 1992), and a cold Mediterranean climate with a mean annual temperature around

11–13 °C and a mean annual rainfall around 500–600 mm, with a summer drought period that occurs every year. The site consisted of sparse populations (about 50 specimens ha$^{-1}$) of isolated mature trees over 100 years old. The species included in the study are *Quercus faginea* (a deciduous species with a mean leaf duration of 5.3 months) and *Q. suber* and *Q. ilex* (two evergreen species with a mean leaf life span of 15 and 23.7 months, respectively) (Mediavilla and Escudero 2003). All selected specimens were adult individuals, with a diameter of the trunk (taken at 1.3 m height) between 40 and 60 cm and a height between 8 and 10 m.

## Leaf morphological, anatomical, and chemical measurements

Ten specimens from each species were selected for morphological and anatomical leaf measurements. By the end of June (fully expansion) 2019, several branches with sunny leaves were taken from each canopy at mid-height at the periphery of the crown. The samples were immediately taken to the laboratory and in the two evergreen species, the branches were separated into annual segments (shoots) of different age classes. Only leaves of the current year were included in the study.

The morphological traits were analyzed in 100 leaves randomly selected from each species (10 leaves per tree). Total projected leaf area (LA, cm$^2$) was determined using image analysis (Delta-T Devices LTD, Cambridge, UK). The samples were oven-dried at 70 °C to constant mass and the total dry mass per leaf was determined. From the data obtained, we calculated the leaf mass per area (LMA, g m$^{-2}$). The data of the 10 leaves selected in each case were averaged to obtain a value per tree. The anatomical traits were measured in 20 leaves for each species (2 leaves in each tree, obtaining then a value for each tree as an average of the data corresponding to the two leaves analyzed in each case).

For histological analysis, 5 × 5 mm pieces were removed from the middle part of the leaves with a razor blade and fixed in formaldehyde-acetic acid (FAA; 35–40% formaldehyde, 70% ethanol and 100% acetic acid, 1:8:1 v/v) for at least 24 h. They were then dehydrated in an ethanol series (starting at 50% and ending at 100%) and embedded in methacrylate liquid for 72 h for later section. After breaking the mold and grinding, leaf transverse sections (5–6 µm thick) were cut using a HM 350S Rotary Microtome (Microm International GmbH, Germany), proceeding later to the sliding of the cut (in methylacetate for 1 h and subsequent dehydration in an ethanol series, from 100 to 50%, and ending with distilled water, for 5 min in each case). The samples were then subjected to hematoxylin/eosin staining, dehydration, starting with distilled water and following through an ethanol series (starting at 50% and ending at 100%), to finish with a xylol rinse (4 passes of 5 min each). Leaf sections were then mounted in glass slides and sealed with neutral glue. Images of each section were obtained with a digital camera (Nikon Sight DS-smc, Nikon Instruments INC, USA) mounted on a microscope (Nikon Eclipse 90i, Nikon Instruments INC, USA) at 100 × magnification. Total leaf thickness (LT, µm), palisade (PT, µm) and spongy mesophyll thickness (ST, µm) and adaxial ($E_{AD}$, µm) and abaxial ($E_{AB}$, µm) epidermal thickness were calculated using the software ImageJ. Two measurements of the total thickness of the leaf and each tissue were taken for each photograph, in all cases at the midpoint between two vascular bundles.

Quantitative measurements of leaf trichomes were made by analyzing images of another subsample of leaves using a scanning electron microscope (SEM EVO HD25, Carl Zeiss Microscopy, Germany) at 20 × magnification. The number of trichomes was counted as the total number of trichome branches, with each branch of stellate trichomes counted as a trichome (Bourland and Hornbeck 2007), and expressed per unit of leaf area (TD, number mm$^{-2}$).

For chemical analyses, a disk of the same size (0.28 cm$^2$) was cut from 10 intact current-year leaves from each of the 10 specimens selected for each species. At the laboratory, the plant material was weighed and immediately plunged into liquid nitrogen and kept at – 80 °C until analysis. For chlorophyll determinations, we used the method of Agrisera (Sweden). Chlorophyll was measured according to Porra et al. (1989). The dry mass and LMA of the leaves used for the analyses were also determined and the chlorophyll (CF) content of leaves was expressed per unit dry mass and per unit leaf area.

## Interception of light by the two leaf surfaces for different angles of inclination of the sun

Between six and ten adult individuals of each species were selected for the study. The crowns had a hemispheric shape with a clustered distribution of leaves. This allowed the identification of individualized branches, which makes it possible to differentiate sets of leaves that function as an independent unit from the point of view of light interception. Three branches of each specimen were pruned after taking photographs to record the exact position in the tree. Sampling positions in the crown were selected to represent the most sun-exposed parts of the canopies. The three positions sampled were south, east, and west. The branches were selected based on the criterion that they faced the sun at the times of day when the sun was positioned in front of the corresponding part of the crown during the days of the year with the highest PPFD intensities and temperatures. The positions of the sun on 1st July at our latitude were: 90° azimuth, 37° elevation for the eastern part of the crown, 180° azimuth, 71° elevation at the south, and – 90° azimuth, 37° elevation at the western position. Branches with these orientations were sampled on each selected specimen.

All the branches contained between 300 and 700 leaves and were of similar length. At the laboratory, the branches were arranged on a tripod, simulating their actual field position. All branches were 3D-digitized using a 3Space Fastrak electro-magnetic device (Polhemus Inc., Colchester, VT, USA), which provided all the measurements required for the three-dimensional reconstruction using the Y-PLANT program (Pearcy and Yang 1996). A single branch per day was collected so that it could be processed as soon as possible to prevent leaf loss. Y-PLANT interprets the plant as a system consisting of a set of nodes which, distributed from the base to the top along the main stem and each of the branches, form the main structure on which new branches or leaves are inserted. Thus, each of these nodes, connected to the previous one by a segment of stem or branch, can be attached to a new stem segment, branch segment or a leaf. The information required by the program for the three-dimensional reconstruction of the canopy includes measurements of several parameters in stems and petioles (diameter, length, azimuth, orientation, and angle from the vertical) and in leaves (length, orientation, azimuth and angle from the horizontal viewed from the adaxial side of the leaf). Using the program, we estimated, for each direction Ω of incident light, defined by zenith and azimuth angle of the sun, the projected leaf area ($PA_\Omega$, the total area of the leaves projected toward a determined direction, depending on the angle and orientation of the leaves), and the displayed area ($DA_\Omega$, obtained by subtracting the leaf area shaded from the projected leaf area). Both areas were calculated for the sun's position at intervals of 30 min on 1st July.

Since PA is the area of all leaves in the viewpoint plane without leaf overlap, whereas DA includes the effects of leaf overlap (self-shading), for each branch and for each direction Ω of incident light, we calculated two estimates of efficiency that depend on the architectural arrangement of foliage: projection efficiency ($Ep_\Omega$, $PA_\Omega$ divided by the total leaf area, TLA) and the Silhouette to Total Area Ratio ($STAR_\Omega$, $DA_\Omega$ divided by TLA, which may be taken as an estimate of leaf display efficiency). In turn, given that:

$$STAR_\Omega = \frac{PA_\Omega}{TLA} \times \frac{DA_\Omega}{PA_\Omega} \tag{1}$$

$PA_\Omega/TLA$ may be interpreted as the leaf inclination component of $STAR_\Omega$ and $DA_\Omega/PA_\Omega$ as the leaf overlapping component (Delagrange et al. 2006). Thus, STAR includes both the effect of leaf angles and the spatial distribution of leaves that influence their self-shading.

We also estimated the average PPFD incident for each individual leaf on the branch. The data were estimated separately for sunlit and shade leaves. For these simulations, we assumed a permanently clear sky, a latitude of 42° N and an atmospheric transmission coefficient of 0.79. Finally, only data corresponding to the hours of the day when sun incidence angles were 0° and 45° with respect to the main axis of each branch were used in this study. With these incidence angles, the selected branches were not shaded by adjacent branches. So, we restricted our measurements to the time of the day when our branches were fully illuminated, since it can be expected that these time periods represent the most part of daily $CO_2$ assimilation by the selected branches. More information about the program can be obtained from Pearcy and Yang (1996, 1998) and Valladares and Pearcy (1998).

## Photosynthetic light–response curves and absorptance measurements

A CIRAS-2 portable photosynthesis system (PP Systems, Amesbury, MA, USA) equipped with leaf gas exchange chamber was used. Measurements were made under controlled conditions. During each session, the instrument was programmed to maintain environmental conditions within the chamber similar to the external values at the measurement time: around 400 ppm $CO_2$ concentration, 20–30 °C air temperature, and 40–60% relative humidity. The light was provided by blue ($\lambda = 455$ nm) and red ($\lambda = 620$ nm) LED diodes. Light saturation curves were performed at the following theoretical PPFD values: 0, 300, 600, 900, 1200, 1500, and 1800 µmol $m^{-2}$ $s^{-1}$. Approximately half of the curves were performed by beginning at the highest irradiance and decreasing to 0 µmol $m^{-2}$ $s^{-1}$ PPFD and the other half at increasing levels of illumination. Both methods yielded similar results. Measurements lasted 30 min at 0 µmol $m^{-2}$ $s^{-1}$ and 15 min in all the intermediate light levels. In most cases, the time intervals used were long enough to obtain stable conductance and assimilation values. Three readings at each level were averaged to obtain reliable values. Measurements were performed on the ten individuals of each species selected for morphological determinations. All measurements were performed on attached fully expanded leaves inserted in the medial zone of the canopy between 0700 and 01600 h local solar time on sunny days during June and July (the period of full canopy display for the three species), through 2 years (2018–2019). The determinations were made during the same day for each specimen, on leaves receiving light on different sides and at different positions along the shoot. Only current-year leaves were used in the two evergreen species. Light absorptance was measured using a Plant Stress Kit (Opti-Sciences, Inc., Hudson, USA) on the same leaves used for gas exchange measurements, by means of RGB sensors (62% blue light, 7% green light, and 31% red light).

## Data analysis

Photosynthetic light response for each leaf is assumed to be expressed by the non-rectangular hyperbola (Thornley 1998):

$$A = \frac{\propto I + A_{\max} - \sqrt{\left(\propto I + A_{\max}\right)^2 - 4 \propto \theta I A_{\max}}}{2\theta} - R_{\mathrm{d}}$$

where $I$ is the incident PPFD, $A_{\max}$ indicates light-saturated photosynthetic rate, $\alpha$ and $\Theta$ indicate the initial slope and the convexity, respectively, and $R_{\mathrm{d}}$ is the dark respiration rate. The photosynthetic light saturation and compensation points were estimated from the light–response curves. Fitting of the curves was performed with SPSS version 26.0 (SPSS Inc., Chicago, IL). Estimations of branch-level $CO_2$ assimilation rates were performed using the PPFD values incident on each individual leaf calculated with Y-PLANT and the light–response curves. Two-way analysis of variance (ANOVA) was used to examine the possible differences between species and leaf sides for all variables estimated.

## Results

### Leaf traits

The three species showed significant differences in individual leaf area, which was highest for the deciduous *Q. faginea* and lowest for *Q. ilex* (Table 1). By contrast, leaf thickness and leaf mass per unit area were lowest in *Q. faginea*. In all cases, the epidermis was thicker in the adaxial than in the abaxial side. The thickness of palisade mesophyll was larger than that of the spongy mesophyll. *Q. faginea* was the species with the largest proportion of the total leaf thickness occupied by epidermis, particularly at the adaxial side, while *Q. suber* had the largest percentage of palisade mesophyll at the expenses of the spongy mesophyll. *Q. suber* was also the species with the highest density of trichomes on the abaxial surface, whereas the two other species did not exhibit significant differences in trichome density (Table 1). Only *Q. ilex* leaves presented trichomes on its adaxial surface, although at very low density compared to the abaxial side. Finally, the chlorophyll content per unit leaf mass significantly decreased across the three species as their leaf longevity increased, but the differences between the two evergreens disappeared when expressed per unit leaf area (Table 1).

### Branch architecture and light interception by the two leaf surfaces for different sun elevation angles

As expected for such complex canopies, the percentage of total leaf area displayed (Silhouette to Total Area Ratio, STAR) was rather low (Table 2). For any position of the

**Table 1** Average leaf traits in three Mediterranean oak species (SE in parentheses, $n = 10$ trees). Only data from the current-year leaf age class in the evergreen species are included. For each leaf trait, means with different letters indicate significant differences between species at P = 0.05 (Tukey test)

| Species | LA | LMA | LT | E ad | E ab | PM | SM | DT ab | DT ad | CF area | CF mass |
|---|---|---|---|---|---|---|---|---|---|---|---|
| *Q. faginea* | 7.97 (0.46) a | 131 (1.81) c | 196 (2.71) c | 22.5 (0.83) b | 10.1 (0.48) a | 95 (1.49) a | 69 (2.22) a | 161 (13) b | – | 1.02 (0.04) a | 7.09 (0.33) a |
| *Q. suber* | 6.45 (0.41) b | 183 (4.65) b | 265 (4.16) b | 14.7 (0.56) a | 8.3 (0.52) b | 165 (2.73) b | 77 (3.08) a | 309 (17) a | – | 0.83 (0.06) b | 4.43 (0.33) b |
| *Q. ilex* | 2.97 ( (0.26) c | 255 (2.45) a | 345 (5.04) a | 28.6 (1.80) c | 9.9 (0.43) ab | 182 (2.74) c | 125 (4.35) b | 173 (24) b | 11 (0.63) | 0.69 (0.05) b | 2.91 (0.24) c |

Abbreviations and units: LA = individual leaf area ($cm^2$); LMA = leaf mass per area ($g\ m^{-2}$); LT = leaf thickness (µm); Ead = thickness of adaxial epidermis (µm); Eab = thickness of abaxial epidermis (µm); SM = thickness of spongy mesophyll (µm); PM = thickness of palisade mesophyll (µm); DT ab = trichome density in abaxial surface (no $mm^{-2}$); DT ad = trichome density in adaxial surface (no $mm^{-2}$); CF mass = Chlorophyll content per unit leaf mass ($mg\ g^{-1}$); CF area = Chlorophyll content per unit leaf area ($g\ m^{-2}$)

sun, STAR tended to be significantly lower in *Q. ilex*, but the interspecific differences were not very accentuated. In all species, for sun incidences near 0° with respect to the main axis of the branch, the proportion of total leaf area illuminated from the abaxial surface was much lower than that of the adaxial surface, especially in *Q. suber*. However, for sun incidence angles of 45° with respect to the orientation of the branch, the percentage of the leaf area illuminated from below was considerable, especially for *Q. faginea*. For both sun positions, *Q. suber* was the species with the highest ratio of adaxial/abaxial exposure to light (Table 2). Leaf projection efficiency ($\mathrm{Ep}_{\Omega}$) was higher for the leaves facing the sun from the adaxial side irrespective of the sun elevation (Table 2). In consequence, mean PPFD received by the sunlit part of the leaf area was always larger at the upper leaf side. The ratio adaxial/abaxial sunlit PPFD tended to be higher for *Q. ilex* than for the two other species, especially for sun incidences of 45°. In correspondence with the lower STAR values of *Q. ilex*, the mean PPFD received by the whole leaf area (including both sunlit and self-shaded fractions of the crown) was low for this species, mainly at the abaxial side.

## Photosynthetic light–response curves

Light–response curves for the three oak species generated by varying light intensities are shown in Fig. 1. Among the three species, *Q. ilex* showed the lowest initial slope of the curve (Table 3). Interspecific differences tended to be less intense when the slope was calculated on an absorbed PPFD basis (not shown), but they were still significant ($P < 0.001$). The light compensation point tended to be higher in *Q. ilex* with respect to the two other species, both in adaxial and abaxial surfaces. *Q. suber* reached intermediate values between the two other species for most photosynthetic parameters, with the exception of dark respiration per unit leaf area, which was highest (more negative) in *Q. suber*.

Between both leaf surfaces, the adaxial side tended to show lower light compensation and saturation points than the lower side (Table 3). The differences in compensation point were not due to differences in dark respiration rates, which were obviously similar in the determinations made on both leaf sides. The initial slope of the curve was significantly higher in the adaxial leaf side than in the abaxial in the three species. Between-sides differences were also

**Table 2** Display ($\mathrm{STAR}_{\Omega}$) and projection ($\mathrm{Ep}_{\Omega}$) efficiency (% of total leaf area per branch) at different sun incidence angles with respect to the main axis of the branch and for adaxial (ad) and abaxial (ab) leaf surfaces in three Mediterranean oak species. Mean branch-level PPFD ($\mu$mol m$^{-2}$ s$^{-1}$) incident on sunlit leaves and average incident PPFD for both sunlit and self-shaded fractions of the crown. Values are mean and standard error (*n*= 20–30 branches). Significance (P) of main effects and interaction

| Parameters | Incidence | Leaf side | *Q. faginea* | *Q. suber* | *Q. ilex* | Species | Leaf side | Sp × leaf side |
|---|---|---|---|---|---|---|---|---|
| $\mathrm{STAR}_{\Omega}$ | 0° | ad | 21.4 (1.47) | 23.5 (1.88) | 18.1 (1.34) | 0.04 | < 0.0001 | NS |
| | 0° | ab | 7.2 (0.63) | 6.2 (0.33) | 5.6 (0.65) | | | |
| | | ad/ab | 2.97 | 3.79 | 3.23 | | | |
| $\mathrm{STAR}_{\Omega}$ | 45° | ad | 12.1 (1.06) | 18.1 (0.74) | 11.8 (0.81) | 0.002 | < 0.0001 | < 0.0001 |
| | 45° | ab | 13.5 (0.30) | 10.6 (0.36) | 9.9 (0.48) | | | |
| | | ad/ab | 0.90 | 1.71 | 1.19 | | | |
| $\mathrm{Ep}_{\Omega}$ | 0° | ad | 58.01 (1.12) | 62.33 (1.46) | 58.33 (1.3) | 0.0016 | < 0.0001 | NS |
| | 0° | ab | 37.61 (0.86) | 41.07 (1.51) | 36.49 (0.94) | | | |
| | | ad/ab | 1.54 | 1.52 | 1.60 | | | |
| $\mathrm{Ep}_{\Omega}$ | 45° | ad | 52.6 (1.27) | 60.17 (0.98) | 54.86 (1.67) | < 0.0001 | < 0.0001 | 0.059 |
| | 45° | ab | 40.04 (0.68) | 42.45 (1.47) | 37.88 (0.87) | | | |
| | | ad/ab | 1.31 | 1.42 | 1.45 | | | |
| PPFD (sun) | 0° | ad | 976 (18) | 1082 (17) | 999 (26) | < 0.0001 | < 0.0001 | NS |
| | 0° | ab | 589 (15) | 649 (35) | 567 (22) | | | |
| | | ad/ab | 1.66 | 1.67 | 1.76 | | | |
| PPFD (sun) | 45° | ad | 950 (22) | 1092 (16) | 1015 (32) | 0.0014 | < 0.0001 | 0.04 |
| | 45° | ab | 691 (16) | 731 (36) | 654 (21) | | | |
| | | ad/ab | 1.37 | 1.49 | 1.55 | | | |
| PPFD (sun + shade) | 0° | ad | 617 (25) | 614 (22) | 498 (24) | < 0.0001 | < 0.0001 | NS |
| | 0° | ab | 344 (16) | 352 (24) | 278 (16) | | | |
| | | ad/ab | 1.79 | 1.74 | 1.79 | | | |
| PPFD (sun + shade) | 45° | ad | 637 (31) | 675 (26) | 559 (27) | < 0.0001 | < 0.0001 | NS |
| | 45° | ab | 442 (25) | 438 (34) | 352 (18) | | | |
| | | ad/ab | 1.44 | 1.54 | 1.59 | | | |

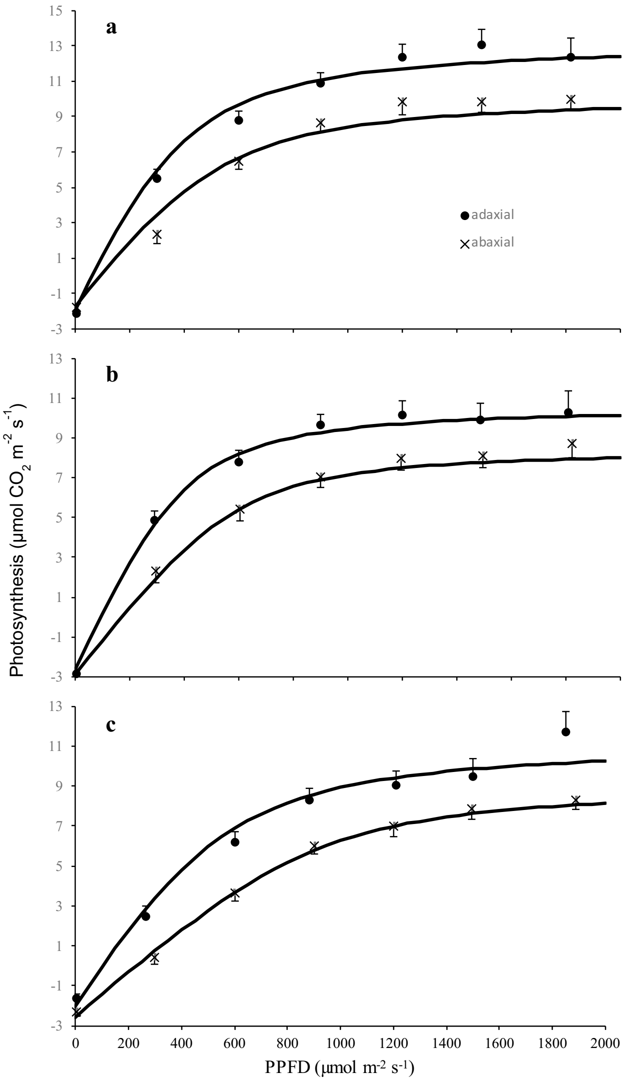

**Fig. 1** The response of net photosynthesis to irradiance incident on the adaxial or abaxial surfaces of **a** *Quercus faginea*, **b** *Q. suber,* and **c** *Q. ilex* leaves. Lines represent predicted values (non-rectangular hyperbola model). Error bars represent 1 SE ($n = 10–20$)

significant ($P = 0.03$) when the slope was calculated on an absorbed PPFD basis (not shown). By contrast, there were no significant differences in the convexity parameter ($\Theta$) between leaf sides. Finally, maximum photosynthesis was always lower on the abaxial with respect to the adaxial surface. The differences between both leaf sides were especially accentuated for the longest-living leaves (29% in *Q. faginea*, 25% in *Q. suber* and 47% in *Q. ilex*), which resulted in interspecific differences that tended to be stronger for the abaxial side, although the interaction term was non-significant. By contrast, similar values of stomatal conductance at full light intensity were seen for both leaf sides.

Since the measurements were made under similar conditions for the different species and for both leaf sides, no significant differences were seen in leaf temperature and air humidity between species, nor between leaf surfaces within each species (data not shown). In consequence, transpiration rates were also similar for both sides of the leaf (not shown). However, there were differences between leaf surfaces for $CO_2$ assimilation rates at light saturation, which resulted in water use efficiency values (WUE) significantly lower for the abaxial side, with more pronounced relative differences between surfaces in the species with longer-living leaves (Table 3), although the interaction term was again non-significant.

The abaxial leaf surface had systematically lower levels of visible light absorptance than the adaxial side (Table 3). The differences in absorptance between the adaxial and the abaxial sides intensified across the three species with the increase in leaf thickness, reaching 20, 33 and 43% in *Q. faginea*, *Q. suber,* and *Q. ilex,* respectively. There were significant differences in absorptance between the three species, with lowest values in *Q. ilex*, both in the adaxial and abaxial sides, although the interspecific differences were more accentuated for the abaxial surface, which led to a significant interaction term between species and leaf side.

## Branch-level $CO_2$ assimilation rates

Average branch-level assimilation rates per unit leaf area during the two selected hours at 1st July were significantly different for the different species (not shown). As expected, the highest values were obtained for *Q. faginea* and the lowest for *Q. ilex*. Logically, within each species, branch-level assimilation rates were lower than light-saturated assimilation rates (Fig. 2), because of the diminished PPFD levels of the different fractions of the crown. Sunlit assimilation rates (expressed as a percentage of the maximum potential photosynthesis) for the leaves receiving light from the upper side were comparatively high for *Q. suber* owing to the high projection efficiencies of this species (Table 2) and lowest for *Q. ilex*. Mean sunlit photosynthetic rates for both leaf sides were comparatively low at 45° incidence angle, because of the high proportion of leaves receiving light from the lower side at these conditions, and comparatively high in *Q. suber* with respect to the two other species at both sun incidences. Mean assimilation rates by the whole leaf area (including both sunlit and self-shaded fractions of the crown) were lowest for *Q. ilex* due to the high degree of self-shading. Mean realized assimilation rate by the whole leaf biomass of each branch was approximately 20% of the maximum potential light-saturated rates in *Q. ilex*, whereas *Q. faginea* and *Q. suber* realized between 37 and 34% of their respective photosynthetic potential.

**Table 3** Mean values (SE in parenthesis, $n = 10–20$) of the different parameters of the photosynthetic light–response curves obtained under adaxial (ad) and abaxial (ab) illumination in three oak species and mean absorptance values for both leaf sides. Significance (P) of main effects and interaction

| Parameters | Leaf surface | *Q. faginea* | *Q. suber* | *Q. ilex* | Species | Leaf side | Sp × leaf side |
|---|---|---|---|---|---|---|---|
| Initial slope | ad | 0.0324 (0.0024) | 0.029 (0.0024) | 0.0203 (0.0021) | < 0.0001 | < 0.0001 | NS |
| (mol $CO_2$ mol PPFD$^{-1}$) | ab | 0.0195 (0.0021) | 0.0175 (0.0032) | 0.0115 (0.0008) | | | |
| | ad/ab | 1.66 | 1.66 | 1.77 | | | |
| Dark respiration rate | ad | − 1.97 (0.21) | − 2.61 (0.29) | − 2.05 (0.22) | 0.01 | NS | NS |
| (μmol $CO_2$ $m^{-2}$ $s^{-1}$) | ab | − 1.74 (0.38) | − 2.9 (0.25) | − 2.57 (0.2) | | | |
| | ad/ab | 1.13 | 0.90 | 0.80 | | | |
| Convexity (Θ) | ad | 0.79 (0.061) | 0.86 (0.046) | 0.82 (0.047) | NS | NS | NS |
| | ab | 0.83 (0.067) | 0.79 (0.054) | 0.91 (0.035) | | | |
| | ad/ab | 0.95 | 1.09 | 0.90 | | | |
| Light compensation point | ad | 62 (6) | 110 (12) | 127 (16) | < 0.0001 | < 0.0001 | 0.01 |
| (μmol photons $m^{-2}$ $s^{-1}$) | ab | 78 (19) | 206 (29) | 243 (19) | | | |
| | ad/ab | 0.79 | 0.53 | 0.52 | | | |
| Light saturation point | ad | 950 (62) | 856 (62) | 1108 (43) | 0.004 | 0.0008 | 0.089 |
| (μmol photons $m^{-2}$ $s^{-1}$) | ab | 1023 (69) | 1183 (105) | 1202 (29) | | | |
| | ad/ab | 0.93 | 0.72 | 0.92 | | | |
| Photosynthesis max | ad | 13.24 (0.82) | 10.65 (0.83) | 11.19 (0.84) | 0.009 | < 0.0001 | NS |
| (μmol $CO_2$ $m^{-2}$ $s^{-1}$) | ab | 10.23 (0.74) | 8.5 (0.92) | 7.62 (0.48) | | | |
| | ad/ab | 1.29 | 1.25 | 1.47 | | | |
| Stomatal conductance max | ad | 172 (14) | 147 (10) | 146 (15) | NS | NS | NS |
| (mmol $H_2O$ $m^{-2}$ $s^{-1}$) | ab | 167 (13) | 143 (14) | 148 (24) | | | |
| | ad/ab | 1.03 | 1.03 | 0.99 | | | |
| WUE | ad | 4.27 (0.23) | 4.73 (0.27) | 4.02 (0.27) | 0.037 | < 0.0001 | NS |
| (μmol $CO_2$ $mmol^{-1}$ $H_2O$) | ab | 3.51 (0.19) | 3.77 (0.26) | 3.08 (0.26) | | | |
| | ad/ab | 1.22 | 1.25 | 1.31 | | | |
| Absorptance | ad | 0.89 (0.0016) | 0.85 (0.0021) | 0.83 (0.0027) | < 0.0001 | < 0.0001 | < 0.0001 |
| (relative units) | ab | 0.74 (0.0042) | 0.63 (0.0061) | 0.58 (0.0046) | | | |
| | ad/ab | 1.20 | 1.35 | 1.43 | | | |

## Discussion

Under the same environmental conditions, values of absorptance and light-saturated photosynthesis were substantially greater under adaxial than under abaxial illumination, confirming the different photosynthetic properties for each surface observed by numerous authors on asymmetric leaves of other species (Terashima 1986; DeLucia et al. 1991; Ustin et al. 2001; Bauerle et al. 2004; Driscoll et al. 2006; Mänd et al. 2013; Lu et al. 2015; Zhang et al. 2016). Other parameters of the response of $CO_2$ assimilation to PPFD, such as the initial slope and compensation and saturation PPFD levels, also significantly differed between both leaf sides. The main consequence of the low Amax and the larger compensation point of the abaxial side is that abaxial illumination implies reduced photosynthetic rates at any light intensity with respect to adaxial illumination (Fig. 1). The differences in assimilation rates between both leaf sides were not due to the differences in stomatal conductance, since under similar light and atmospheric conditions, there were no differences in stomatal conductance and transpiration rates between leaves illuminated from below with respect to adaxial illumination. This coincides with the results obtained by other authors (Poulson and DeLucia 1993; Valladares and Pearcy 1999; Peguero-Pina et al. 2009), which suggests that lower assimilation rates under abaxial illumination reflect the complex interactions of light with leaf optical properties, rather than direct stomatal effects (DeLucia et al. 1991). Receiving light from below alters the light gradient within the leaf by the difference in optical properties between palisade and spongy tissues (Terashima and Saeki 1985; Terashima 1986; Myers et al. 1997). The high absorbance of chlorophyll in the spongy tissue (Brodersen and Vogelmann 2010) means that light received from the underside barely penetrates the palisade tissue, which represents most of the photosynthetic volume of the leaf. It has also been proposed that the abaxial sides of leaves are more susceptible to high radiation damage in

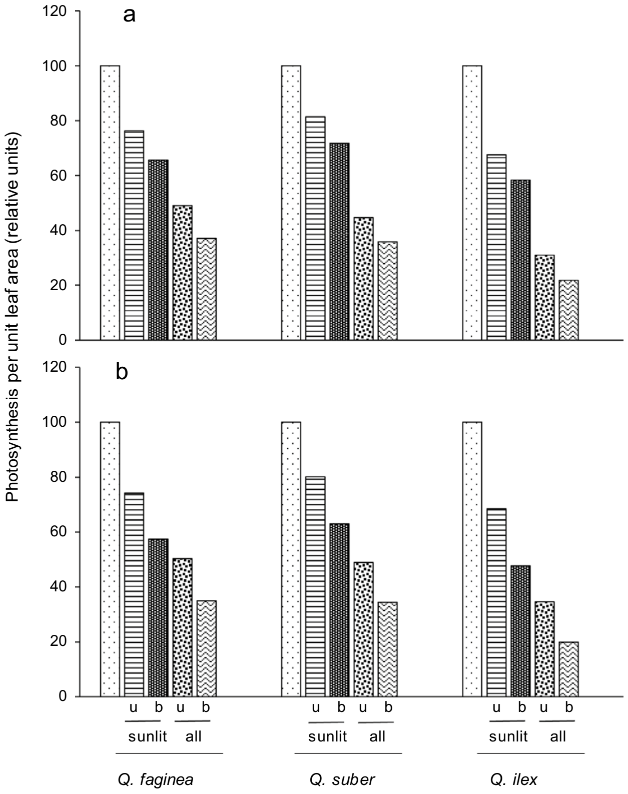

**Fig. 2** Estimated average assimilation rates for sun incidence angles of **a** 0° and **b** 45° expressed as a percentage of the maximum adaxial light-saturated photosynthesis per unit leaf area of each species (Amax, punctuated bars) in the different fractions of the foliage for three Mediterranean oak species. u: mean branch-level assimilation for the leaves facing the sun by the upper side. b: mean branch-level assimilation for both leaf orientations. Sunlit: mean branch-level assimilation for the leaves receiving direct solar radiation. All: mean branch-level assimilation for both sunlit and self-shaded fractions of the crown

contrast to the adaxial. The palisade tissue, due to its lower absorptance, allows reduced light absorption and, because its cells function as conduits for light, this can allow the penetration of light to photosynthetic tissues deep within the leaf without reaching photoinhibitory levels (Terashima and Saeki 1983; Sun et al. 1998; Vogelmann and Evans 2002). Lower absorptance may thus reduce the risk of photodamage. A partial photoinhibition of the most upper chloroplasts in the palisade parenchyma cells, which still absorb and dissipate light energy, can protect the remaining leaf chloroplasts from photoinhibition and enable photosynthesis rates fairly normal in the deeper layers of the leaf (Lichtenthaler et al. 2005).

However, our study revealed that these differences between leaf surfaces tended to be of different magnitude for the different species. The relative variation of absorptance, light-saturated assimilation, initial quantum yield, and compensation point on the abaxial with respect to the adaxial surface tended to be stronger for *Q. ilex* than for the two other species, although the interaction term between species and leaf side was not always significant. These interspecific trends are probably the consequence of the differences in leaf traits that accompany the changes in leaf life span. The greater thickness and LMA and lower chlorophyll content per unit mass of longer-lived leaves of *Q. ilex* are associated with lower light uptake and lower initial response slope to increased radiation in comparison with leaves with shorter duration, regardless of the illuminated leaf surface. Since both the light microenvironment and the chlorophyll content and light absorption decline with leaf depth toward the abaxial side (Terashima and Saeki 1985; Knapp et al. 1988; Vogelmann 1993; Evans 1995), also the greater thickness typical of longer-lived leaves should contribute to create deeper gradients from ad- to abaxial leaf surfaces. On the other hand, differences in absorptance have been attributed primarily to differences in reflectance among leaf surfaces, with higher reflectance values on the abaxial surface, because of its larger aerial interspaces between the mesophyll cells and a consequently greater extent for light reflectance processes (Syvertsen and Cunningham 1979; DeLucia et al. 1991; Cordón and Lagorio 2007; Lu et al. 2015). Lighter abaxial leaf surfaces or “bicoloration” (Slaton et al. 2001; Hatier and Gould 2007) is mainly the result of the greater reflectance by the spongy tissues in bifacial leaves (Terashima et al. 2009). Among our species, the contrast in coloration between adaxial and abaxial surfaces was low in *Q. faginea* and particularly intense in *Q. ilex* (Fig. 3), which would indicate that in this last species, the contrast between the reflectance of the abaxial surface and the adaxial surface is greater, and therefore, the decrease in absorptance between both surfaces is also larger. Although some authors have provided data that seem to suggest that trichomes would not modify radiation penetration (Proietti and Palliotti 1997), others do attribute a role to the density of hairs in the reflectance values at visible wavelengths for leaf surfaces (Syvertsen and Cunningham 1979; Morales et al. 2002; Lu et al. 2015; Bickford 2016). In our case, however, differences in pubescence did not determine the differences in absorptance between leaf surfaces, since the marked contrast in the coloration of both surfaces in *Q. ilex* occurred despite the fact that this species showed a density of trichomes on the abaxial side similar to that of the deciduous *Q. faginea*. In turn, *Q. suber* showed less differences in absorptance between both leaf sides than *Q. ilex*, despite the fact that *Q. suber* showed the highest trichome density in our study. By contrast, the interspecific differences in absorptance between both surfaces were consistent with the differences in thickness of spongy mesophyll, which may be explained by the greater light scattering ability in leaves with thick spongy mesophyll layer (Peguero-Pina et al. 2009).

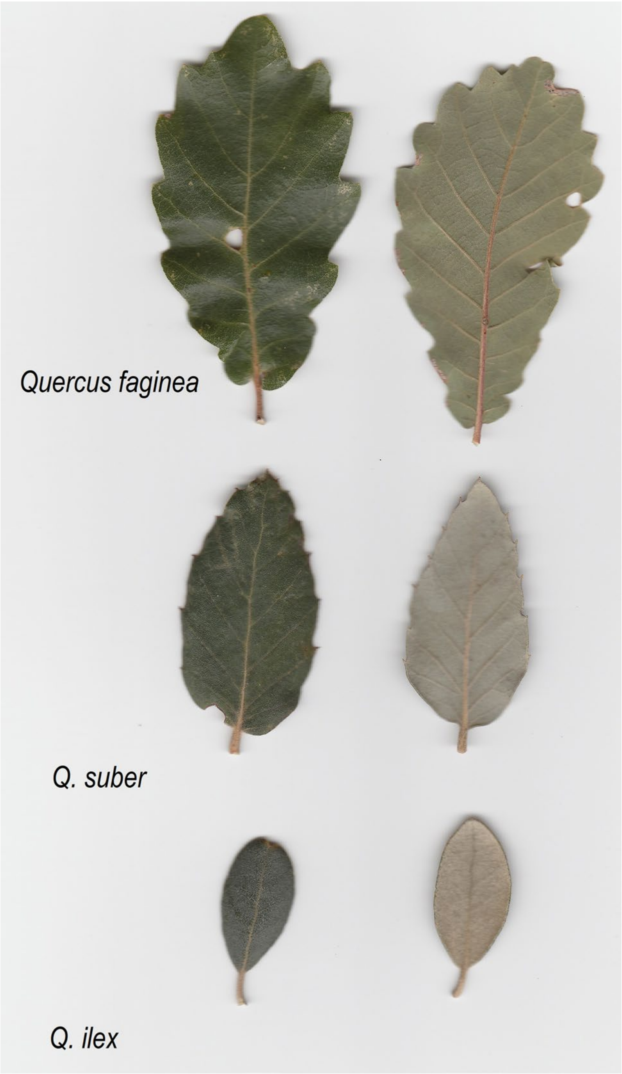

**Fig. 3** Images of adaxial (left) and abaxial (right) leaf surfaces of *Quercus faginea*, *Q. suber,* and *Q. ilex*

As a result of these interspecific differences in the deterioration of the photosynthetic activity on the abaxial surface, the interspecific differences in photosynthetic performance should intensify when the leaves are illuminated from the lower side. This would mean that a spatial arrangement of leaves that involves receiving light to a greater extent on the abaxial surface would be more disadvantageous for *Q. ilex*, because the thick spongy layer in this species contributes to further decreasing C assimilation potential under abaxial illumination in comparison with the other species. On the other hand, a thick spongy layer might be favorable for increasing $CO_2$ assimilation under certain conditions, because of the increase in absorptance due to light diffusion (detour effect). Under conditions of shade, light is enriched in the wavelengths less efficiently absorbed by the photosynthetic apparatus, and the gain in absorptance by the detour effect for these wavelengths may be considerable, which should contribute to an increase in C gain in the inner fractions of the leaf biomass (Terashima et al. 2009).

*Q. ilex* was the species with the lowest percentage of the total leaf area displayed (STAR) for any position of the sun, because a large number of leaves per unit branch area more than compensated for the small individual leaf area of this species (Escudero et al. 2017). The high levels of self-shading in *Q. ilex* resulted in significantly lower mean branch-level PPFD values for the whole leaf area (Table 2). In Mediterranean climates during the growing season, PPFD often exceeds the saturation value for fully exposed leaves and this excess radiation is often detrimental to leaf survival (Pintó-Marijuan and Munné-Bosch 2014). Specifically, in cold Mediterranean climates, such as in the present study, these limiting situations for photosynthesis can occur both during the summer and winter months (Corcuera et al. 2005), in which high and low temperatures, respectively, restrict photosynthetic capacity and the energy absorbed cannot be fully utilized. Photoprotection mechanisms become particularly important in such circumstances and especially in longer-lived leaves where premature loss of leaf area is more costly in terms of leaf-level $CO_2$ fixation than in leaves with shorter duration. Branch architectural patterns may be interpreted as structural mechanisms for minimizing excessive amounts of radiation (Valladares and Pugnaire 1999; Werner et al. 2001; Pearcy et al. 2005) and may then constitute an effective strategy in adverse environments (Werner et al. 2001). The low STAR values in *Q. ilex* may thus be explained as an increase in structural protection necessary for an evergreen species, although we expected that also the evergreen *Q. suber* should exhibit lower STAR values than the deciduous *Q. faginea*, in contrast with the results obtained. The negative consequence of a high degree of self-shading may be quantified by comparing the difference between the mean $CO_2$ assimilation rates obtained for the sunlit part of the crown and the mean rates estimated for the whole leaf area (Fig. 2), which was especially accentuated for *Q. ilex*, in correspondence with the low mean PPFD values incident per unit leaf area for this species (Table 2).

The three species also showed differences in the contribution of the abaxial surface to the total displayed leaf area. Our results suggest that the canopy of the three species shows a design oriented to reduce the amount of light received on the abaxial leaf surface for sun incidences near 0° with respect to the main axis of the branch, but for higher incidence angles, the percentage of leaves illuminated from below was considerable, which should contribute to a decrease in the C fixation rates of the leaf biomass, especially in species with strong differences between both leaf surfaces. In addition, for those leaves receiving light from below, projection efficiency ($Ep_{\Omega}$) was significantly lower than for leaves with the upper surface oriented toward the sun. The main consequence of this low $Ep_{\Omega}$ is that the mean PPFD received by the sunlit part of the abaxial surface was significantly lower than that of the adaxial side. In part, this attenuation of the direct light received in the abaxial side may contribute to reducing the risk of photoinhibitory damage, but, combined with the higher compensation point of the leaves under abaxial illumination, mean that a substantial part of the leaf area illuminated from below may be near the minimum light required for a positive C balance, which may further reduce mean assimilation of the canopy. The consequences of abaxial illumination for branch-level photosynthesis may be estimated from the differences between assimilation rates estimated only for the leaves illuminated from the adaxial side and the corresponding values for all leaves on the branch (Fig. 2). This reduction was especially accentuated for the estimations made with an incidence angle of 45°, owing to the large percentage of the leaf area illuminated from below, and especially for *Q. ilex*, because of the high compensation point for the abaxial side in this species. Among the three species, *Q. suber* exhibited the highest display efficiencies, as well as the most elevated projection efficiencies. At the same time, this species exhibited the lowest proportions of the leaf area illuminated from below. This would suggest that the branch architecture in this species is especially efficient in terms of light interception. This translated in values of realized photosynthesis at the branch level similar to those of *Q. faginea*, thus compensating the elevated light compensation points and reduced maximum quantum yield of the leaves of *Q. suber*. Differences in branch architecture, then, may affect total $CO_2$ assimilation not only through changes in levels of self-shading (Falster and Westoby 2003; Duursma et al. 2012), but also through its effects on the percentage of leaves illuminated from below.

Obviously, the assimilation rates estimated in the present paper should be taken only as an approximation to the true canopy-level assimilation rates. The description of branch architecture is an extremely time-consuming task (Delagrange et al. 2006; Sinoquet et al. 2007). It is almost impossible to perform all the measurements needed for a thorough description of a large crown. Accordingly, the architectural characteristics seen in the present paper are only valid for the particular branches selected and cannot, in principle, be extrapolated to the entire canopy. However, the interspecific differences in architectural patterns seem to be strong enough to determine the significant interspecific differences in the light interception patterns. Similarly, the assimilation rates of the three species were significantly different, although our estimates are only valid for the time periods when the response curves were performed. It is known that photosynthetic rates in a seasonal environment experience large variations in parallel with the seasonal changes in soil and atmospheric conditions. In addition to architectural differences, there were interspecific differences in leaf size and shape (Fig. 3), which may have significant effects on gas exchange through changes in boundary layer conductance. Smaller leaves tend to have a thinner boundary layer (Scoffoni et al. 2011), but lobed leaves may also allow for increased air turbulence and thereby decrease the boundary air layer (Schuepp 1993). These possible differences between the three species cannot be detected by the measurements made within a leaf chamber. It is also known that collimated light that strikes a leaf obliquely at low angles may be less effective for photosynthesis than light that strikes the leaf perpendicularly (Brodersen and Vogelmann 2010). The probable effect of including these differences would be further decreasing assimilation rates of those leaves with lower projection efficiency. Given that leaves that received light from the abaxial side had less projection efficiency, this effect should further increase the assimilation reduction in the leaves illuminated from below.

Finally, since gas exchange measurements were made with red-blue light, the responses under solar illumination may be different to those obtained by us, because of the higher absorptance values of red and blue wavelengths. By contrast, absorptance measurements were made with RGB sensors. Given our uncertainty with respect to the actual absorptance values, we have preferred to calculate the photosynthetic responses on an incident, instead of absorbed, light basis. Accordingly, the final estimates of branch-level assimilation rates were also calculated with respect to incident light. Our results show that photosynthetic levels for a given incident PPFD were lower on the abaxial with respect to the adaxial side and that the between-side differences were of different magnitude for the three species, which significantly affected the average branch-level assimilation rates of the different species. We postulate that the main reason for these differences is the interspecific difference in the absorptance values for the abaxial side.

## Conclusions

Photosynthetic performance was lower under abaxial illumination for the three species. However, the deterioration of assimilatory potential in the lower surface tended to be stronger in *Q. ilex*. A probable explanation for this difference was the lower absorptance of the lower side in leaves with thick spongy mesophyll. The differences between leaf sides contributed decisively to reducing branch-level C fixation. Average realized photosynthesis tended to be highest (in comparison with the potential maximum) for the deciduous species, and lowest for the evergreen with longer leaf life span. The deterioration of photosynthetic activity under abaxial illumination would involve an additional cost of the longer-lived leaves which may increase the differences in potential instantaneous assimilation rates seen among species differing in leaf life span (Wright et al. 2002, 2004). Whether the interspecific differences observed among our three species are the consequence of a general trend across species differing in leaf thickness should be tested with a larger set of species, because of their potential impact for the competitive equilibrium between different tree species.

**Author contributions** Both authors contributed to the study conception and design.

**Funding** This paper has received financial support from the Spanish Ministerio de Ciencia e Innovación—EU-FEDER (Project No. CGL2016-79861-P).

**Data availability** Data generated or analyzed during the current study are included in this published article and are available from the corresponding author on reasonable request.

## Declarations

**Conflict of interest** The authors declare no conflict of interest.

## References

Bauerle WL, Weston DJ, Bowden JD, Dudley JB, Toler JE (2004) Leaf absorptance of photosynthetically active radiation in relation to chlorophyll meter estimates among woody plant species. Sci Hort 101:169–178

Bickford CP (2016) Ecophysiology of leaf trichomes. Funct Plant Biol 43:807–814

Bourland FM, Hornbeck JM (2007) Variation in marginal bract trichome density in upland cotton. J Cotton Sci 11:242–251

Brodersen CR, Vogelmann TC (2010) Do changes in light direction affect absorption profiles in leaves? Funct Plant Biol 37:403–412

Campbell P, Middleton EM, McMurtrey JE, Chappelle EW (2007) Assessment of vegetation stress using reflectance or fluorescence measurements. J Env Qual 36:832–845

Chen Q, Baldocchi D, Gong P, Dawson T (2008) Modeling radiation and photosynthesis of a heterogeneous savanna woodland landscape with a hierarchy of model complexities. Agric for Meteor 148:1005–1020

Corcuera L, Morales F, Abadía A, Gil-Pelegrín E (2005) The effect of low temperature on the photosynthetic apparatus of *Quercus ilex* subsp. *ballota* at its lower and upper altitudinal limits in the Iberian Peninsula and during a single freezing-thawing cycle. Trees 19:99–108

Cordón GB, Lagorio MG (2007) Optical properties of the adaxial and abaxial faces of leaves. Chlorophyll fluorescence, absorption and scattering coefficients. Photochem Photobiol Sci 6:873–882

Delagrange S, Montpied P, Dreyer E, Messier C, Sinoquet H (2006) Does shade improve light interception efficiency? A comparison among seedlings from shade-tolerant and -intolerant temperate deciduous tree species. New Phytol 172:293–304

DeLucia EH, Shenoi HD, Naidu SL, Day TA (1991) Photosynthetic symmetry of sun and shade leaves of different orientations. Oecologia 87:51–57

Dorronsoro F (1992) El medio físico-químico: suelos. In: Gómez-Gutiérrez JM (ed) El Libro de las Dehesas Salmantinas. Junta de Castilla y León, Salamanca, pp 71–124

Driscoll SP, Prins A, Olmos E, Kunert KJ, Foyer CH (2006) Specification of adaxial and abaxial stomata, epidermal structure and photosynthesis to $CO_2$ enrichment in maize leaves. J Exp Bot 57:381–390

Duursma RA, Falster DS, Valladares F, Sterck FJ, Pearcy RW, Lusk CH, Sendall KM, Nordenstahl M, Houter NC, Atwell BJ, Kelly N, Kelly JWG, Liberloo M, Tissue DT, Medlyn BE, Ellsworth DS (2012) Light interception efficiency explained by two simple variables: a test using a diversity of small-to medium-sized woody plants. New Phytol 193:397–408

Escudero A, Del Río T, Sánchez-Zulueta P, Mediavilla S (2017) Ontogenetic changes in crown architecture and leaf arrangement: effects on light capture efficiency in three tree species differing in leaf longevity. Ecol Res 32:595–602

Evans JR (1995) Carbon fixation profiles do reflect light absorption profiles in leaves. Aust J Plant Physiol 22:865–873

Evans JR, Jakobsen I, Ögren E (1993) Photosynthetic light-response curves. 2. Gradients of light absorption and photosynthetic capacity. Planta 189:191–200

Falster DS, Westoby M (2003) Leaf size and angle vary widely across species: What consequences for light interception? New Phytol 158:509–525

Fleck S, Niinemets U, Cescatti A, Tenhunen JD (2003) Three dimensional lamina architecture alters light-harvesting efficiency in *Fagus*: a leaf-scale analysis. Tree Physiol 23:577–589

Gil-Pelegrín E, Sanz MA, Cuadrat JM, Peguero-Pina JJ, Sancho-Knapik D (2017) Oaks under Mediterranean-type climates: functional response to summer aridity. In: Gil-Pelegrín E, Peguero-Pina JJ, Sancho-Knapik D (eds) Oaks physiological ecology. Exploring the functional diversity of genus *Quercus* L. Springer, Cham, pp 137–193

Hatier JHB, Gould KS (2007) Black coloration in leaves of *Ophiopogon planiscapus* 'Nigrescens'. Leaf optics, chromaticity, and internal light gradients. Funct Plant Biol 34:130–138

Knapp AK, Vogelmann TC, McClean TM, Smith WK (1988) Light and chlorophyll gradients with *Cucurbita* cotyledons. Plant Cell Environ 11:257–326

Lichtenthaler HK, Buschmann C, Knapp M (2005) How to correctly determine the different chlorophyll fluorescence parameters and the chlorophyll fluorescence decrease ratio $R_{Fd}$ of leaves with the PAM fluorometer. Photosynthetica 43:379–393

Lu S, Lu X, Zhao W, Liu Y, Wang Z, Omasa K (2015) Comparing vegetation indices for remote chlorophyll measurement of white poplar and Chinese elm leaves with different adaxial and abaxial surfaces. J Exp Bot 66:5625–5637

Mänd P, Hallik L, Peñuelas J, Kull O (2013) Electron transport efficiency at opposite leaf sides: effect of vertical distribution of leaf angle, structure, chlorophyll content and species in a forest canopy. Tree Physiol 33:202–210

Mediavilla S, Escudero A (2003) Photosynthetic capacity, integrated over the lifetime of a leaf, is predicted to be independent of leaf longevity in some tree species. New Phytol 159:203–211

Mediavilla S, Escudero A (2023) Branch architecture in relation to canopy positions in three Mediterranean oaks. Oecologia 201:915–927

Mediavilla S, Escudero A, Heilmeier H (2001) Internal leaf anatomy and photosynthetic resource-use efficiency: interspecific and intraspecific comparisons. Tree Physiol 21:251–259

Mediavilla S, Martín I, Babiano J, Escudero A (2019) Foliar plasticity related to gradients of heat and drought stress across crown orientations in three Mediterranean *Quercus* species. PLoS ONE 14(10):e0224462

Mediavilla S, Martín I, Escudero A (2020) Vein and stomatal traits in leaves of three co-occurring *Quercus* species differing in leaf life span. Eur J for Res 139:829–840

Morales F, Abadía A, Abadía J, Montserrat G, Gil-Pelegrín E (2002) Trichomes and photosynthetic pigment composition changes: responses of *Quercus ilex* subsp. *ballota* (Desf.) Samp. and *Quercus coccifera* L. to Mediterranean stress conditions. Trees 16:504–510

Myers DA, Jordan DN, Vogelmann TC (1997) Inclination of sun and shade leaves influences chloroplast light harvesting and utilization. Physiol Plant 99:395–404

Niinemets U, Al Fas N, Cescatti A, Pellis A, Ceulemans R (2004) Petiole length and biomass investment in support modify light interception efficiency in dense poplar plantations. Tree Physiol 24:141–154

Paradiso R, Marcelis LFM (2012) The effect of irradiating adaxial or abaxial side on photosynthesis of rose leaves. In: Hemming S Heuvelink E (eds) VII international symposium on light in horticultural systems. Acta Hort, vol 956, pp 157–163

Pearcy RW, Yang W (1996) A three-dimensional crown architecture model for assessment of light capture and carbon gain by understory plants. Oecologia 108:1–12

Pearcy RW, Yang W (1998) The functional morphology of light capture and carbon gain in the redwood-forest understory plant, *Adenocaulon bicolor* Hook. Funct Ecol 12:543–552

Pearcy RW, Muraoka H, Valladares F (2005) Crown architecture in sun and shade environments: assessing function and tradeoffs with a three-dimensional simulation model. New Phytol 166:791–800

Peguero-Pina JJ, Gil-Pelegrín E, Morales F (2009) Photosystem II efficiency of the palisade and spongy mesophyll in *Quercus coccifera* using adaxial/abaxial illumination and excitation light sources with wavelengths varying in penetration into the leaf tissue. Photosynthesis Res 99:49–61

Pintó-Marijuan M, Munné-Bosch S (2014) Photo-oxidative stress markers as a measure of abiotic stress-induced leaf senescence: advantages and limitations. J Exp Bot 65:3845–3857

Porra RJ, Thompson WAA, Kriedemann PE (1989) Determination of accurate extinction coefficients and simultaneous equations for assaying chlorophylls a and b extracted with four different solvents: verification of the concentration of chlorophyll standards by atomic absorption spectroscopy. Biochim Biophys Acta (BBA) Bioenerget 975:384–394

Poulson ME, DeLucia EH (1993) Photosynthetic and structural acclimation to light direction in vertical leaves of *Silphium terebinthinaceum*. Oecologia 95:393–400

Proietti P, Palliotti A (1997) Contribution of the adaxial and abaxial surfaces of olive leaves to photosynthesis. Photosynthetica 33:63–69

Schuepp P (1993) Tansley review no. 59. Leaf Bound Layers New Phytol 125:477–507

Scoffoni C, Rawls M, McKown A, Cochard H, Sack L (2011) Decline of leaf hydraulic conductance with dehydration: relationship to leaf size and venation architecture. Plant Physiol 156:832–843

Sinoquet H, Stephan J, Sonohat G, Lauri PE, Monney P (2007) Simple equations to estimate light interception by isolated trees from canopy structure features: assessment with three-dimensional digitized apple trees. New Phytol 175:94–106

Slaton MR, Hunt ER, Smith WK (2001) Estimating near-infrared leaf reflectance from leaf structural characteristics. Am J Bot 88:278–284

Smith WK, Vogelmann TC, Delucia EH, Bell DT, Shepherd KA (1997) Leaf form and photosynthesis: do leaf structure and orientation interact to regulate internal light and carbon dioxide? Bioscience 47:785–793

Sun J, Nishio JN (2001) Why abaxial illumination limits photosynthetic carbon fixation in spinach leaves. Plant Cell Physiol 42:1–8

Sun J, Nishio JN, Vogelmann TC (1998) Green light drives $CO_2$ fixation deep within leaves. Plant Cell Physiol 39:1020–1026

Syvertsen JP, Cunningham GL (1979) The effects of irradiating adaxial and abaxial 162 leaf surface on the rate of net photosynthesis of *Perezia nana* and *Helianthus annuus*. Photosynthetica 13:287–293

Terashima I (1986) Dorsiventrality in photosynthetic light response curves of a leaf. J Exp Bot 37:399–405

Terashima I, Saeki T (1983) Light environment within a leaf. 1. Optical properties of paradermal sections of *Camellia* leaves with special reference to differences in the optical properties of palisade and spongy tissues. Plant Cell Physiol 24:1493–1501

Terashima I, Saeki T (1985) A new model for leaf photosynthesis incorporating the gradients of light environment and of photosynthetic properties of chloroplasts within a leaf. Ann Bot 56:489–499

Terashima I, Fujita T, Inoue T, Chow WS, Oguchi R (2009) Green light drives leaf photosynthesis more efficiently than red light in strong white light: revisiting the enigmatic question of why leaves are green. Plant Cell Physiol 50:684–697

Thornley JHM (1998) Dynamic model of leaf photosynthesis with acclimation to light and nitrogen. Ann Bot 81:421–430

Ustin SL, Jacquemoud S, Govaerts Y (2001) Simulation of photon transport in a three-dimensional leaf: implications for photosynthesis. Plant Cell Environ 24:1095–1103

Valladares F, Niinemets U (2007) The architecture of plant crowns: from design rules to light capture and performance. In: Pugnaire FI, Valladares F (eds) Handbook of functional plant ecology. CRC, Boca Raton, pp 101–149

Valladares F, Pearcy RW (1998) The functional ecology of shoot architecture in sun and shade plants of *Heteromeles arbutifolia* M. Roem., a Californian chaparral shrub. Oecologia 114:1–10

Valladares F, Pearcy RW (1999) The geometry of light interception by shoots of *Heteromeles arbutifolia*: morphological and physiological consequences for individual leaves. Oecologia 121:171–182

Valladares F, Pugnaire FI (1999) Tradeoffs between irradiance capture and avoidance in semi-arid environments assessed with a crown architecture model. Ann Bot 83:459–469

Vogelmann TC (1993) Plant tissue optics. Ann Rev Plant Physiol Mol Biol 44:231–251

Vogelmann TC, Evans JR (2002) Profiles of light absorption and chlorophyll within spinach leaves from chlorophyll fluorescence. Plant Cell Environ 25:1313–1323

Vogelmann TC, Nishio JN, Smith WK (1996) Leaves and light capture: light propagation and gradients of carbon fixation within leaves. Trends Plant Sci 1:65–70

Wang Y, Noguchi KO, Terashima I (2008) Distinct light responses of the adaxial and abaxial stomata in intact leaves of *Helianthus annuus* L. Plant Cell Environ 31:1307–1316

Werner C, Ryel RJ, Correia O, Beyschlag W (2001) Structural and functional variability within the canopy and its relevance for carbon gain and stress avoidance. Acta Oecol 22:129–138

Wright IJ, Westoby M, Reich PB (2002) Convergence towards higher leaf mass per area in dry and nutrient-poor habitats has different consequences for leaf life span. J Ecol 90:534–543

Wright IJ, Reich PB, Westoby M, Ackerly DD, Baruch Z, Bongers F, Cavender-Bares J, Chapin T, Cornelissen JHC, Diemer M, Flexas J, Garnier E, Groom PK, Gulias J, Hikosaka K, Lamont BB, Lee T, Lee W, Lusk C, Midgley JJ, NavasML NU, Oleksyn J, Osada N, Poorter H, Poot P, Prior L, Pyankov VI, Roumet C, Thomas SC, Tjoelker MG, Veneklaas EJ, Villar R (2004) The worldwide leaf economics spectrum. Nature 428:821–827

Zhang ZS, Li YT, Gao HY, Yang C, Meng QW (2016) Characterization of photosynthetic gas exchange in leaves under simulated adaxial and abaxial surfaces alternant irradiation. Sci Rep 6:1–11